

Surface-plasmon resonance as a sensitive optical probe of metal-film properties

W. H. Weber and S. L. McCarthy

Scientific Research Staff, Ford Motor Company, Dearborn, Michigan 48121

(Received 7 May 1975)

The resonance excitation of surface plasmons, detected by the scattered-light method, is used in a number of experiments on Ag, Au, and Cu films. These include (i) the determination of optical constants, (ii) the use of a multilayered structure allowing sequential excitation of plasmons on both surfaces of a film, (iii) the study of interference between bulk- and surface-plasmon scattered light, and (iv) the demonstration of surface anisotropy on films grown with the metal vapor beam striking the substrate at an oblique angle. The optical-constant measurements, which were done on the substrate interface, agree with data on bulk samples prepared and measured in vacuum and with film data by Dujardin and Thèye, but they disagree with film data by Schulz and by Johnson and Christy. In samples grown on 77-K substrates a strong increase in bulk scattering is observed which interferes with the roughness-coupled plasmon signal producing a dispersive line shape rather than the usual Lorentzian.

I. INTRODUCTION

The resonant excitation of surface plasmons is a novel and very sensitive probe of the optical properties of highly reflecting metal films. The purpose of this paper is to demonstrate the use of this probe in a number of experiments on noble metals. Included in these experiments are (i) the determination of optical constants, (ii) the use of a multilayered structure allowing the sequential excitation of plasmons on both surfaces of a film, (iii) the study of the interference between bulk- and surface-plasmon scattered light, and (iv) the demonstration of surface anisotropy on films grown with the metal vapor beam striking the substrate at an oblique angle of incidence. In general, the information yielded by the resonance method in each of the above experiments would be more difficult to obtain using conventional reflection and transmission measurements.

Measurements of the optical dielectric function $\epsilon(\omega)$ of the noble metals in the visible portion of the spectrum have been made since the beginning of the century. The experimental techniques which have been used include reflectivity measurements on bulk and opaque thin-film samples and a combination of reflection and transmission studies on semitransparent thin films.¹ The qualitative features of the data, which are adequately explained as arising from a combination of free-electron and interband effects, show reasonable agreement among the wide variety of experiments. There are serious discrepancies, however, if one compares the actual values for the optical constants reported by different authors. One would expect these discrepancies to disappear as better measurement and sample-preparation techniques are developed, but this has not always been the case. For example, the recent measurements on semitransparent films of $\text{Re}(\epsilon)$ by Johnson and Christy²

in the 650-nm region agree with previous data by Schulz³ on similar Au and Cu films, but disagree with the bulk measurements on vacuum-prepared surfaces by Otter⁴ and Roberts.⁵ The magnitude of the discrepancy is 10 to 40 times larger than the experimental uncertainty, depending upon which author's values are used for this quantity. On the other hand, the data by Hodgson⁶ and Thèye⁷ on Au films and Dujardin and Thèye⁸ on Ag films are in agreement with Otter's bulk data, indicating that film and bulk samples can yield the same optical constants.

For obtaining precision optical constants the surface-plasmon resonance technique is useful only in the region of the spectrum for which $-\text{Re}(\epsilon) \gg \text{Im}(\epsilon)$, which is a region bounded at high frequencies by the onset of interband transitions and at low frequencies by the condition $\omega\tau \gg 1$, where τ is the familiar optical relaxation time from the Drude theory. Limitations on accuracy restrict the useful region even further in our experiments to $-\text{Re}(\epsilon) \leq 50-100$. This means that the method is restricted to highly reflecting metals in a limited spectral region. Within these limitations, however, very precise values for $\epsilon(\omega)$ can be obtained, since the accuracy depends upon measuring angles and refractive indices, rather than intensities, and the results are not very sensitive to the film thickness. In our experiments the surface plasmons are excited at the interface between the metal film and a fused-quartz substrate, thus minimizing contamination and surface-roughness effects. Previous reflectivity measurements on Au films⁶ and plasmon resonance measurements on Ag films⁹ indicate that the two surfaces of a film can have different optical constants.

In Sec. II, a brief review of the surface-plasmon technique is given along with the pertinent equations. Section III contains the experimental details for film growth and resonance measurements, and

Sec. IV gives the results. In Sec. V we present detailed comparisons between our measurements of $\text{Re}(\epsilon)$ and those of other authors for which numerical data are available. Although both the real and imaginary parts of ϵ are determined, the real part is much less sensitive to film-grain size and annealing history⁷ and, therefore, is subject to more meaningful comparisons.

II. SURFACE-PLASMON RESONANCE

The first demonstration of the resonant excitation of surface plasmons was by Otto¹⁰ in 1968. He observed the attenuated total reflection (ATR) of a light beam reflected from the inside surface of a prism in close proximity to a silver film. Turbadar¹¹ actually discovered the effect a decade earlier but did not associate it with surface plasmons. In the ATR method, which has subsequently been used in several studies of surface waves in metals and semiconductors,¹²⁻¹⁷ the internal reflectivity is measured as a function of frequency for fixed prism angle or as a function of angle for fixed frequency. In either case the coupling to the surface plasmon is usually across an air gap or other low-index dielectric layer. Kretschmann and Raether showed that the resonance could also be observed by measuring the scattered light (SL) from the surface plasmon due to surface roughness.^{18,19} The SL method, which we use in our experiments, has several advantages over ATR: (i) The coupling can be done through the metal film whose thickness can be measured and controlled more accurately than the air gap often used for ATR; (ii) the SL experiments can be easily performed in the weak-coupling limit with fairly thick films using a sensitive detector, since there is little or no background signal. In the same limit the ATR method requires measuring a small change in a large background signal and (iii) the direct recording of resonance curves is generally simpler in the SL method. This is particularly true when a monochromatic beam is used which is tuned through the resonance by changing the angle of incidence. The main limitation of the SL method is that sources of scattered light other than the surface plasmon must be discriminated against.

The dispersion relation for surface plasmons excited at the interface between a metal film of thickness d with complex dielectric constant ϵ_2 and a substrate with dielectric constant ϵ_3 is given by¹⁰

$$\epsilon_2 k_3 + \epsilon_3 k_2 + \frac{\epsilon_1 k_2 + i \epsilon_2 k_1}{\epsilon_1 k_2 - i \epsilon_2 k_1} (\epsilon_2 k_3 - \epsilon_3 k_2) e^{-2k_2 d} = 0, \quad (1)$$

where

$$k_1 = (\epsilon_1 \omega^2 / c^2 - k_{sp}^2)^{1/2}, \quad k_2 = (k_{sp}^2 - \epsilon_2 \omega^2 / c^2)^{1/2}, \\ k_3 = (k_{sp}^2 - \epsilon_3 \omega^2 / c^2)^{1/2},$$

and ϵ_1 is the dielectric constant of the medium on the other side of the metal, which in our case is an index-matching fluid coupling the film to the prism. The phases of all the square roots are chosen so that the k 's have positive real parts.

We excite the resonances by varying the angle of incidence θ of a monochromatic beam incident from medium one. Thus Eq. (1) should be viewed as a relation giving the complex surface-plasmon wave vector k_{sp} as a function of the real frequency ω . Near resonance, the amplitude $A(\theta)$ of the plasmon field can be represented by a simple pole:

$$A(\theta) \propto (k_{||} - k_{sp})^{-1} = [(\omega/c)n_p \sin\theta - k_{sp}]^{-1}, \quad (2)$$

where $k_{||}$ is the projection of the incident wave vector onto the prism-film interface and n_p is the prism index. The scattered intensity is proportional to $|A(\theta)|^2$, yielding a Lorentzian line shape whose peak position θ_m and half-width at half-maximum $\Delta\theta$ are given by

$$\text{Re}(k_{sp}) = (\omega/c)n_p \sin\theta_m, \quad (3)$$

$$\text{Im}(k_{sp}) = (\omega/c)n_p \cos\theta_m \Delta\theta. \quad (4)$$

Note that the dispersion relation (1) is an exact formula which includes radiation and absorption damping of the plasmon and the effects due to finite film thickness. For a given set of experimental data, which includes refractive index values as well as measurements of θ_m , $\Delta\theta$, and d , Eq. (1) yields a unique complex value for ϵ_2 . This value is determined by a computer program which uses Newton's method with complex variables to solve Eq. (1). Although approximate expressions for ϵ_2 can be used in certain cases,^{12,19} these were generally not accurate enough. The computer program was also used to determine the uncertainty of each value for ϵ_2 .

III. EXPERIMENTAL

Films of Ag, Au, and Cu were grown by electron-beam evaporation using 99.999%-pure starting material in an oil-free ion-pumped vacuum system. Pressures during the growth were typically in the 1×10^{-7} Torr range, and the growth rates were 1-2 nm/sec. Film thicknesses were 70-90 nm, and these were measured to ± 3 nm by interferometric techniques. Fused-silica substrates $25 \times 50 \times 1$ mm³ with a commercial optical polish were used. These were ultrasonically cleaned before being placed in the vacuum system and then cleaned by ion bombardment prior to film deposition. The substrate temperature could be controlled between 77 and 300 K.

The prism used for optical-constant measurements on the substrate-interface plasmons was a 30°-60°-90° right-angle prism made from Schott SF-6 glass. The metal films were mounted against

the large surface of the prism with an index-matching fluid, and the beam was incident on the surface making a 60° angle with the film. We were not able to use a fluid which exactly matched the prism index $n_p \approx 1.8$, since fluids with indices in this range contain methylene iodide, which has a tendency to attack noble-metal films. The highest index fluid which we were able to use was α -iodonaphthalene with an index ≈ 1.7 . The index mismatch produced a small interference modulation on some of the resonance curves, but this did not seriously affect the accuracy of the measurements.

The prism is mounted on a motor-driven rotating table as shown in Fig. 1. An angular position signal, used for the x -axis of an X - Y recorder, is obtained with a 25-turn potentiometer coupled to the driving shaft. A monochromatic, collimated, p -polarized, light beam from a He-Ne laser, a He-Cd laser, or from one of the spectral lines of a high pressure Hg lamp is aligned to intersect at right angles the axis of rotation of the table. The scattered-light signal is detected by an RCA-7265 photomultiplier tube which views the back of the substrate through a 1-m-long flexible-optical-fiber cable, one end of which is rigidly attached to the prism-table assembly.

Since the diameter of the cable is comparable to that of the incident beam, i. e., several millimeters, it is important that in the vicinity of a resonance the beam does not move across the film as the table is rotated. Referring to Fig. 1, we see that this condition requires

$$\left. \frac{dx}{d\alpha} \right|_{\alpha=\alpha_m} = 0, \quad (5)$$

where x is given by

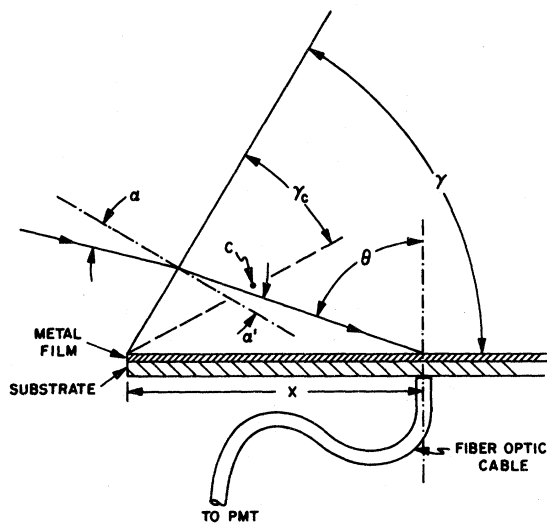


FIG. 1. Geometry for the surface-plasmon excitation and detection.

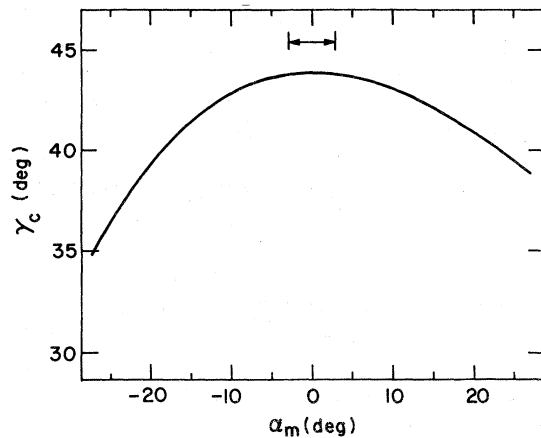


FIG. 2. Solution to Eq. (5) for the prism used in the optical-constant measurements. The solid arrow indicates the full range of experimental α_m values.

$$x(\alpha) = L \cos \gamma_c \cos \alpha' (1 - \tan \gamma_c \tan \alpha) / \cos(\gamma + \alpha'), \quad (6)$$

α_m corresponds to the peak in the resonance curve, L is the distance of the axis of rotation C from the 60° corner of the prism, γ is the prism angle, γ_c is the angle between the 60° face and the axis of rotation, α is the entrance angle, and α' is related to α by Snell's law, $n_p \sin \alpha' = \sin \alpha$.

For given values of α_m , γ , and n_p , Eq. (5) yields a unique value of γ_c , which determines the position of the prism. Changing the wavelength changes α_m and, in general, would require a repositioning of the prism. We have avoided this problem, however, by choosing the prism angle and index so that the resonances all occur at small values of α , i. e., near normal incidence on the front surface of the prism. Expanding Eq. (5) for small α , we find that

$$\gamma_c = \arctan(\tan \gamma / n_p), \quad (7)$$

which is independent of α to first order. This result is demonstrated in Fig. 2, where we show the solution to Eq. (5) using the actual prism parameters at $\lambda = 632.8$ nm. The range of experimental values is also indicated, where the lower limit corresponds to the 690.7-nm Ag resonance and the upper one to the 632.8-nm Au resonance. An additional advantage of choosing the resonances to occur at small α values is that all angles can be measured relative to $\alpha = 0$, and this point can be indexed accurately ($\pm 1'$) by observing the beam reflected back through the collimating optics off the front surface of the prism.

The prism angle for the SF-6 prism was measured to be $59^\circ 56' 30'' \pm 40''$ and the refractive index values were determined from data supplied by the manufacturer for the glass blank used to make the prism. The reported accuracy of these numbers

is $\pm 1 \times 10^{-4}$. As an independent check, we determined $n_p(\lambda)$ at several wavelengths by measuring the angle of minimum deviation, and these values agreed with the Schott data to within the accuracy of our measurements ($\pm 2 \times 10^{-4}$). The substrate refractive indices were determined from published data²⁰ on high-purity fused silica with an accuracy an order of magnitude better than that for the prism. Measurements were also done on the air surface of the metal films by mounting the substrate side of the samples against a 45° Crown glass prism.

IV. RESULTS

A. Optical constants

The complex dielectric constants of Ag, Au, and Cu were determined on films grown at 300 K by exciting plasmons on the metal-substrate interface. An example of the data is shown in Fig. 3 for a 70-nm Ag film. From curves such as those in Fig. 3, the resonance peak positions α_m and halfwidths $\Delta\alpha$ are measured directly. The angle θ is related to α by $\theta = \gamma + \sin^{-1}(\sin\alpha/n_p)$, thus the complex k_{sp} values are determined using Eqs. (2) and (3). The optical constants of the metal are then found by solving Eq. (1) for each value of k_{sp} . The uncertainty in the peak positions is approximately $\pm 0.1^\circ$, while the uncertainty in their widths is about $\pm 5\%$. Similar data are obtained for Cu and Au films, but only the 690.7 and 632.8 nm wavelengths could be used since $-\text{Re}(\epsilon)$ is smaller for these metals.

A summary of our measurements is given in Table I. Each value of ϵ represents the average of three different samples grown simultaneously. The uncertainties $\delta\text{Re}(\epsilon)$ and $\delta\text{Im}(\epsilon)$ are estimated by calculating the square root of the sum of the

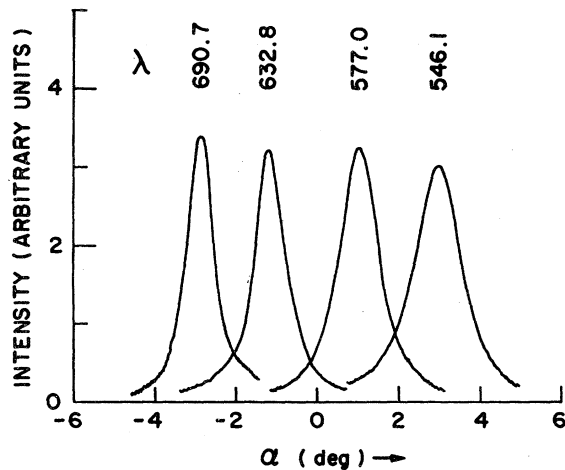


FIG. 3. Surface-plasmon resonance data for a 70-nm Ag film. The wavelength of the light is indicated above each curve.

squares of the errors introduced by each variable, e.g.,

$$\delta\text{Re}(\epsilon) = \left[\sum_{i=1}^6 \left(\frac{\partial\text{Re}(\epsilon)}{\partial\eta_i} \delta\eta_i \right)^2 \right]^{1/2}, \quad (8)$$

where the η_i are the various experimental quantities and $\delta\eta_i$ are their estimated uncertainties: $\delta d = 3$ nm, $\delta\alpha_m = 0.1^\circ$, $\delta\Delta\alpha = 5\%$, $\delta n_p = 1 \times 10^{-4}$, $\delta n_s = 1 \times 10^{-5}$, $\delta\gamma = 40''$. The uncertainties in α_m and $\Delta\alpha$ give the major contributions, by at least a factor of 2, to the errors in $\text{Re}(\epsilon)$ and $\text{Im}(\epsilon)$, respectively. These uncertainties could be reduced by expanding the α scale and carefully fitting the resonance curves to the exact line shapes, rather than using the Lorentzian approximation. Such a procedure appears to be unwarranted, however, since the sample-to-sample variation is presently nearly as large as the uncertainties listed in Table I.

As λ increases, $-\text{Re}(\epsilon)$ increases, and the surface-plasmon dispersion curve moves closer to the light line of the adjacent dielectric. Thus, at larger wavelengths the surface plasmon becomes less sensitive to the optical properties of the metal and begins to look like a photon traveling parallel to the surface. This feature is reflected in Table I by the increased uncertainty in $\text{Re}(\epsilon)$ at the longest wavelength.

Measurements were generally made on a sample within an hour of its removal from the vacuum system. Films kept for several weeks in a vacuum desiccator showed little or no change in their optical constants at the substrate interface, even though the air surface sometimes showed visible discoloration. Vacuum annealing at 100 – 200°C for several hours also did not change the substrate interface data.

B. Excitation of two plasmons on one film

A metal film can always support two separate surface-plasmon modes which, in the thick-film limit, correspond to a plasmon localized primarily on one surface or the other. Both of these modes can be observed in a single experiment if the metal film is covered with a thick film of a low-index material before being contacted to the prism. Abelès and Lopez-Rios²¹ have demonstrated this

TABLE I. Summary of optical constants $\epsilon(\omega)$ for the noble metals measured by surface-plasmon resonance.

λ (nm)	Ag	Au	Cu
690.7	-23.40 (± 0.28) +0.864i (± 0.066)	-18.21 (± 0.16) +1.003i (± 0.062)	-19.98 (± 0.20) +0.893i (± 0.051)
632.8	-19.02 (± 0.18) +0.642i (± 0.049)	-13.34 (± 0.075) +0.960i (± 0.055)	-14.67 (± 0.10) +0.724i (± 0.040)
577.0	-15.17 (± 0.10) +0.541i (± 0.039)		
546.1	-13.14 (± 0.073) +0.446i (± 0.031)		

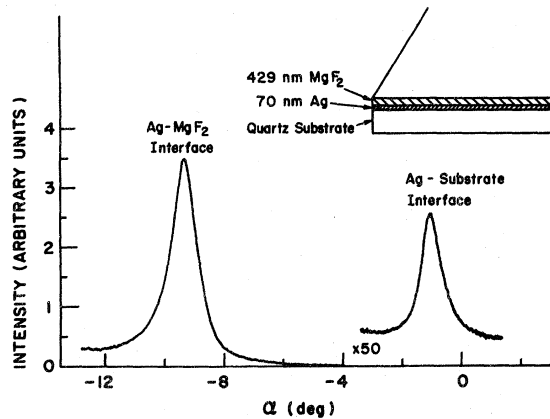


FIG. 4. Sequential excitation of both surface plasmons on a Ag film using $\lambda = 632.8$ nm.

effect in an ATR experiment. As we show below, the SL method works equally well for detecting both plasmons. The low-index layer serves the same purpose as the air gap in the ATR method.

Figure 4 shows the results on a 70-nm Ag film overcoated with a 429-nm MgF_2 layer ($n = 1.38$). The intense resonance at $\alpha = 9.3^\circ$ corresponds to the Ag- MgF_2 surface plasmon, while the weak one at $\alpha = 1.06^\circ$ to the Ag-substrate plasmon. The presence of the MgF_2 layer greatly reduces the coupling to the plasmon on the Ag-substrate interface, resulting in a much weaker signal for that resonance. In principle, using a somewhat more complicated dispersion relation than Eq. (1), the curves in Fig. 4 could be analyzed to yield values for ϵ_2 at each surface of the film.

C. Bulk scattering

The SL method also measures the bulk scattering, which produces a background signal interfering with the roughness-coupled plasmon signal. In films grown on 300-K substrates this background is roughly two orders of magnitude below the plasmon signal and has no observable effect on the resonance line shape. In samples grown on 77-K substrates, however, the background can be nearly as large as the normal signal, leading to a profound change in the observed resonance curve. Figure 5 shows an example of this interference effect which we observed on an 80-nm gold film grown on a 77-K substrate. The background of scattered light away from the resonance is roughly 10^2 times larger in the 77-K grown sample than it was in a similar sample grown at 300 K, also shown in the figure. In addition, the plasmon resonance has a dispersive line shape rather than the usual Lorentzian. The increased background signal away from the resonance is probably due to bulk scattering from a large density of grain boundaries which often occur in samples grown in cold substrates.

The dispersive line shape in Fig. 5 is the result of adding the scattered amplitudes from the driving field, which decays exponentially away from the surface next to the prism, and that from the plasmon field, which decays exponentially away from the surface closest to the detector. The driving field produces the background scattering whose amplitude and phase remain nearly constant in the vicinity of the resonance. The plasmon field, however, undergoes a 180° phase change as well as a large amplitude change near resonance. The phase difference between the two fields can be determined by inspection of the reflection coefficient r_{23} for the H field at the metal-air interface

$$r_{23} = (\epsilon_3 k_2 - \epsilon_2 k_3) / (\epsilon_3 k_2 + \epsilon_2 k_3),$$

where the quantities have the same meaning as in Eq. (1) except that the subscript 3 refers to air. Ignoring the imaginary part of ϵ_2 and the d dependence of k_{sp} , we expand r_{23} in the neighborhood of θ_m to obtain

$$r_{23} = \frac{-A}{(\omega/c)n_p \sin\theta - k_{sp}},$$

where A is a positive constant given by

$$A = \frac{2k_3^2}{k_{sp}(1 + \epsilon_3 k_3 / \epsilon_2 k_2)}.$$

When $(\omega/c)n_p \sin\theta < k_{sp}$, r_{23} is positive and the H component of the plasmon field is in phase with the driving field. The measured signal results from light scattered primarily in the direction normal to the film surface. This light arises from the

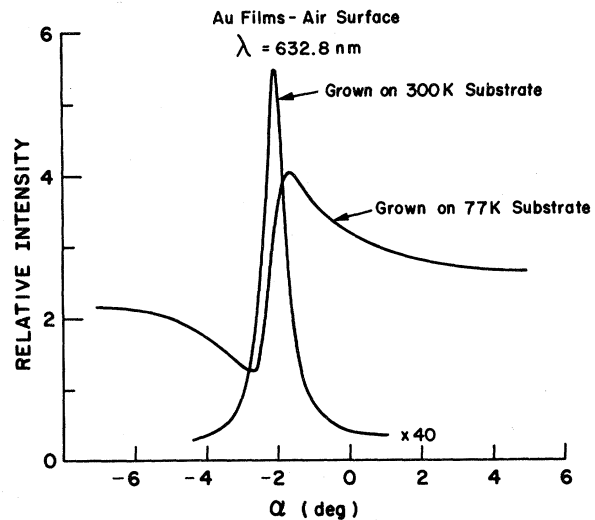


FIG. 5. Interference effect observed on the air surface of an 80-nm Au film grown on a 77-K substrate. A Crown glass prism is used with $\gamma = 44^\circ 57' 30''$ and $n_p = 1.51434$. The gain is $40\times$ larger for the sample grown on a 300-K substrate.

tangential component of the electric field, which has exactly the opposite phase, relative to the driving field as the H field. This means that we should expect destructive interference for $(\omega/c)n_p \sin\theta < k_{sp}$ and constructive interference for $(\omega/c)n_p \sin\theta > k_{sp}$, i. e., a dip on the low-angle side of k_{sp} and an increase on the high-angle side, which is consistent with our observations. Note that the phase change for light propagating across the film is negligible, so that all the scattered radiation can be considered to originate in the same plane.

The completely dispersive line shape in Fig. 5 is an extreme example that occurs only when the bulk signal is at least as large as the plasmon signal. Typically the background interference, which was only observable on 77-K grown films, produced a slightly asymmetric resonance line which was steeper on the low-angle side and had a shoulder on the high-angle side. The only striking difference in the optical constants between Ag and Au films grown at 77 K and those grown at 300 K was a 25% smaller value for $\text{Im}(\epsilon)$ in the 77-K-grown Ag films measured at the substrate interface. This result was surprising since one would generally expect smaller grain sizes and, therefore, larger values for $\text{Im}(\epsilon)$ in samples grown on cold substrates.

D. Surface anisotropy

Noble-metal films evaporated onto smooth glass or quartz substrates tend to grow as small crystallites with a $\langle 111 \rangle$ fiber texture.^{7,22} With oblique incidence deposition, the axes of the fibers at the free surface tend to point toward the beam rather than normal to the surface. The result will be a

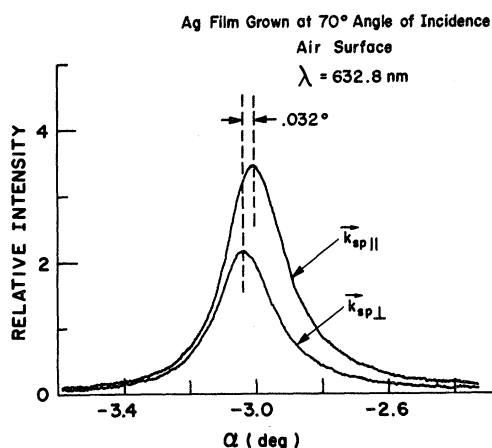


FIG. 6. Surface anisotropy observed on the air surface of a 70-nm Ag film using the same prism as that in Fig. 5. $k_{sp\perp}$ means that the direction of propagation of the plasmon is perpendicular to the direction the metal vapor beam was incident on the substrate during growth. $k_{sp\parallel}$ is 90° from $k_{sp\perp}$. The difference in intensities is a real effect.

porous surface region with a preferred structural direction. The dielectric constant of such a structure can be treated by representing the surface as a collection of oriented metallic ellipsoids and then using a Maxwell-Garnett type averaging of the air and metal dielectric constants.²³ Since the polarizability of the ellipsoids depends on the direction of the field, the effective dielectric constant of the surface region measured by the plasmon resonance method will depend on the propagation direction of the surface plasmon.

In order to observe this anisotropy we chose to investigate Ag films, since this metal produces the narrowest resonances. An example of the data, using a greatly expanded angular scale, is shown in Fig. 6 for a 70-nm Ag film grown at 70° oblique incidence. The direction of propagation of the plasmon relative to the surface orientation is changed by rotating the substrate on the prism without moving the prism or changing the spot at which the beam hits the sample. Although the positions of the resonances change by as much as $\pm 0.1^\circ$ between samples, the shift between k_{sp} parallel and perpendicular to the growth direction for any one sample is reproducible to $\pm 0.007^\circ$. The 50% increase in scattered intensity for $k_{sp\parallel}$ was also quite reproducible. The difference between the effective optical constants resulting from an analysis of the curves in Fig. 6 corresponds to a normal-incidence reflectivity difference of 1.5×10^{-4} , which indicates the sensitivity of the method.

V. COMPARISON WITH OTHER OPTICAL DATA

In this section we compare our optical data with those from other authors. Since theoretical calculations for the noble-metal optical constants are now available, it is important to establish which experimental techniques, if any, yield data which are consistent with each other to within the experimental errors. Our comparisons are limited, of course, to those authors who have reported numerical data on the $\text{Re}(\epsilon)$ within the narrow spectral range of our data.

Figures 7(a)–7(c) show comparisons of $\text{Re}(\epsilon)$ for Ag, Au, and Cu, respectively. We would expect the results of Otter⁴ and Roberts⁵ to be most representative of pure bulk material since they both did *in situ* vacuum reflectivity measurements on bulk samples. Johnson and Christy,² Schulz,³ Thèye,⁷ and Dujardin and Thèye⁸ used a combination of reflection and transmission on semitransparent films. Error bars are drawn in the figures only when the uncertainty exceeds the size of the point.

Since the film surface-plasmon measurements, the bulk reflectivity measurements, and the film measurements by Thèye and by Dujardin and Thèye show good agreement among themselves, we have drawn smooth curves in the figures to roughly ap-

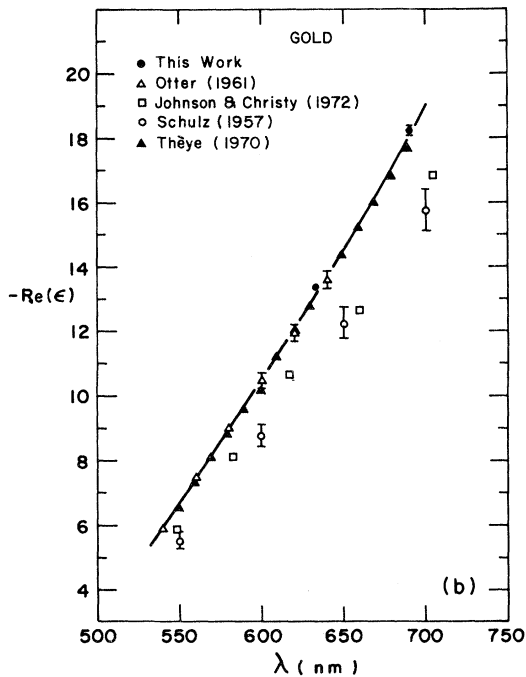
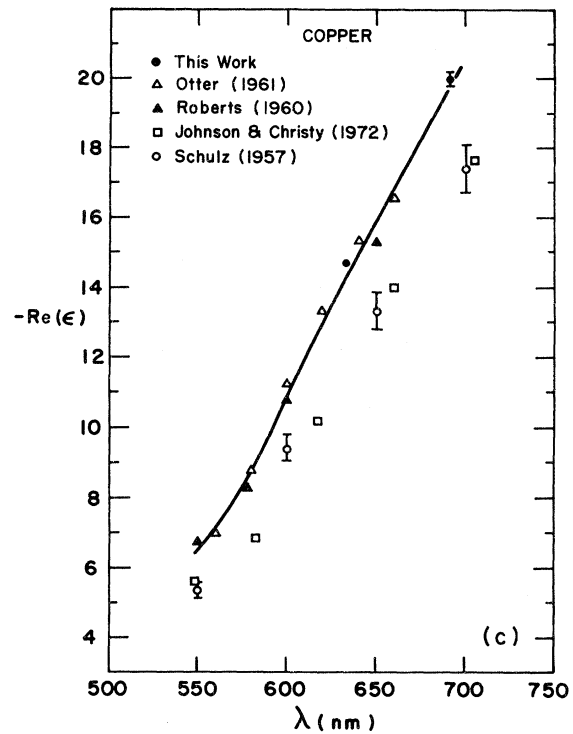
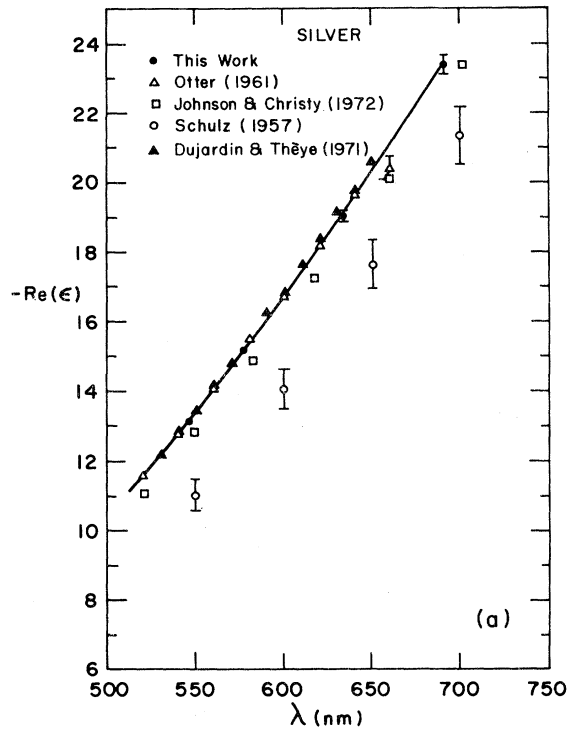


FIG. 7. Comparison of $-\text{Re}(\epsilon)$ measured by various authors. Otter (Ref. 4) and Roberts (Ref. 5) did bulk, *in situ*, vacuum measurements; the remainder are film measurements. The numerical data referred to Thèye (Ref. 7) and to Dujardin and Thèye (Ref. 8) were provided through a private communication and are not contained in the original references.

is very likely contributing to the discrepancy.⁵ However, for Ag and Au the discrepancy is probably due more to a difference in the surface structure of the samples, since there is no known contaminant that can form on these metals during the time of the measurements, and some measurements on exposed surfaces of annealed films have yielded bulk data. This suggestion is supported by the fact that our surface-plasmon measurements on the exposed surface of all three metals yielded values for $-\text{Re}(\epsilon)$ below the curves in the figures. These data showed much more scatter than the substrate-interface data, and they tended to fall between the film measurements by Schulz and Johnson and Christy. In addition, Hodgson found that internal reflectivity on opaque Au films reproduced Otter's bulk data, while external reflection on the same films yielded smaller values for $-\text{Re}(\epsilon)$.

ACKNOWLEDGMENTS

The authors thank Dr. J. Lambe for suggesting the measurements with films grown on 77-K substrates. The samples were provided by M. L.

proximate their average as a function of wavelength. In every case the other film measurements fall below these curves. The discrepancy is largest for Cu and smallest for Ag, but it is always much larger than the experimental uncertainty. For the case of Cu, surface contamination from CuO

Parsons and E. B. Schermer. We also thank Dr. M. L. Thèye for sending us copies of Refs. 17 and

21 as well as the numerical data on Ag and Au which are shown in Figs. 7(a) and 7(b).

-
- ¹P. O. Nilsson, *Solid State Phys.* **29**, 139 (1974). This paper contains an extensive review of the experimental literature prior to 1974.
- ²P. B. Johnson and R. W. Christy, *Phys. Rev. B* **6**, 4370 (1972).
- ³L. G. Schulz, *J. Opt. Soc. Am.* **44**, 357 (1954).
- ⁴M. Otter, *Z. Phys.* **161**, 163 (1961).
- ⁵S. Roberts, *Phys. Rev.* **118**, 1509 (1960).
- ⁶J. N. Hodgson, *J. Phys. Chem. Solids* **29**, 2175 (1968).
- ⁷M. L. Thèye, *Phys. Rev. B* **2**, 3060 (1970).
- ⁸M. M. Dujardin and M. L. Thèye, *J. Chem. Phys. Solids* **32**, 2033 (1971).
- ⁹W. H. Weber and S. L. McCarthy, *Appl. Phys. Lett.* **25**, 396 (1975).
- ¹⁰A. Otto, *Z. Phys.* **216**, 398 (1968).
- ¹¹T. Turbadar, *Proc. Phys. Soc. Lond.* **73**, 40 (1959).
- ¹²E. Kretschmann, *Z. Phys.* **241**, 313 (1971).
- ¹³A. S. Barker, Jr., *Phys. Rev. Lett.* **28**, 892 (1972).
- ¹⁴R. W. Gammon and E. D. Palik, *J. Opt. Soc. Am.* **64**, 350 (1974).
- ¹⁵A. J. Braundmeier and E. T. Arakawa, *J. Phys. Chem. Solids* **35**, 517 (1974).
- ¹⁶A. S. Barker, Jr., *Phys. Rev. B* **8**, 5418 (1973).
- ¹⁷F. Abelès and T. Lopez-Rios, in *Proceedings of the First Taormina Research Conference on the Structure of Matter*, 1972, Taormina, Italy, edited by Elias Burstein and Francesco De Martini (Pergamon, New York, 1974), p. 241.
- ¹⁸E. Kretschmann and H. Raether, *Z. Naturforsch. A* **23**, 2135 (1968).
- ¹⁹R. Bruns and H. Raether, *Z. Phys.* **237**, 98 (1970).
- ²⁰American Institute of Physics Handbook, 3rd ed., edited by D. E. Gray (McGraw-Hill, New York, 1972), Chap. 6, p. 28.
- ²¹F. Abelès and T. Lopez-Rios, *Opt. Commun.* **11**, 89 (1974).
- ²²K. L. Chopra, *Thin Film Phenomena* (McGraw-Hill, New York, 1969), pp. 220–221.
- ²³R. W. Tokarsky and J. P. Marton, *J. Appl. Phys.* **45**, 3047 (1974).